2022

Identification and Characterization of the TSSK6 Activating Co-chaperone (TSACC) Gene in Skeletal Muscle

Tala Shourbagi Tello
n01182320@unf.edu

Identification and Characterization of the TSSK6 Activating Co-chaperone (TSACC) Gene in Skeletal Muscle

By

Tala Shourbagi Tello

A thesis submitted to the Department of Biology

in partial fulfillment of the requirements for the degree of

Master of Science in Biology

UNIVERSITY OF NORTH FLORIDA

COLLEGE OF ARTS AND SCIENCES

July 2022

CERTIFICATE OF APPROVAL

The thesis “Identification and Characterization of the TSSK6 Activating Co-chaperone (TSACC) Gene in Skeletal Muscle” submitted by Tala Tello

Approved by the thesis committee: Date

_____ _____

Dr. David Waddell, Ph.D.
Committee Chairperson

_____ _____

Dr. Frank Smith, Ph.D.

_____ _____

Dr. John Hatle, Ph.D.

Table of Contents

Part I: Introduction and Background

Skeletal muscle and skeletal muscle atrophy 1

The Ubiquitin Proteasome System (UPS) 1

Differential Gene Expression in Response to Denervation-induced Atrophy 2

Myogenic Regulatory Factors (MRFs) are upregulated during Muscle Differentiation and Atrophy 6

Mitogen Activated Protein Kinase (MAPK) Signaling 7

AKT signaling cascade 8

Part II: Identification and characterization of TSSK6 Activating Co-chaperone (Tsacc) in skeletal muscle

Overview of Tsacc 10

Materials and Methods 10

Results 17

Tsacc is induced during neurogenic atrophy 17

Tsacc expression is regulated by Myogenic Regulatory Factors 18

Tsacc is alternatively spliced in skeletal muscle cells 19

Tsacc is upregulated during muscle cell differentiation 21

Tsacc full length (FL) and Tsacc-novel display distinct localization patterns in muscle cells 22

Ectopic expression of Tsacc-FL attenuates muscle cell differentiation while Tsacc-novel overexpression has no effect on muscle cell differentiation 24

Overexpression of Tsacc may inhibit AKT activation 27

Discussion 29

Future Directions 31

Characterize the role of Tsacc in the MAP kinase signaling pathway 31

References 34

List of Figures

Figure 1. Schematic of the ubiquitin proteasome system 2

Figure 2. MuRF1 and MAFbx are upregulated during muscle atrophy 3

Figure 3. Transcriptional activity of the MuRF1 gene locus and MAFbx in WT and MuRF1 KO mice post-denervation 5

Figure 4. Process of muscle cell development is controlled by myogenic regulatory factors (MRFs). 7

Figure 5. Schematic of the MAPK signaling pathways 8

Figure 6. The insulin-like growth factor 1 (IGF1)-Akt pathway controls muscle growth via mammalian target of rapamycin (mTOR) and FoxO proteins 9

Figure 7. Tsacc is induced in response to denervation-induced skeletal muscle atrophy 18

Figure 8. Cloning and analysis of the proximal regulatory region of the Tsacc gene locus 20

Figure 9. Schematic of the validated Tsacc transcript and a newly discovered Tsacc novel transcript 20

Figure 10. qPCR analysis of Tsacc expression in C_2C_{12} cells 22

Figure 11. Tsacc-FL localizes to the cytoplasm of muscle cells 23

Figure 12. Tsacc-novel localizes to both the cytoplasm and nucleus of muscle cells 23

Figure 13. Validation of myc-tagged Tsacc-FL and Tsacc-novel overexpression in C_2C_{12} cells 24

Figure 14. Ectopic expression of Tsacc-FL attenuates muscle cell differentiation 26

Figure 15. Ectopic expression of Tsacc-novel does not appear to affect muscle cell differentiation 27

Figure 16. Ectopic expression of either Tsacc-FL or Tsacc-Novel appears to inhibit AKT activation in muscle cells 26

Figure 17. Ectopic expression of Tsacc-novel appears to upregulate the ERK1/2 branch of the MAPK signaling cascade 32

List of Tables

Table 1. List of primers used in this study 12

Table 2. List of antibodies used in this study 16

Abstract

Skeletal muscle atrophy is defined as a decrease in muscle size and occurs due to disparate physiological conditions, including aging, immobilization, and corticosteroid exposure. TSSK6 activating co-chaperone (TSACC) was identified as a gene that is significantly upregulated in skeletal muscle in response to denervation. To confirm Tsacc expression in skeletal muscle, the Tsacc cDNA was cloned from cultured myoblast cells leading to the discovery of a novel alternative splice-variant that is 49 amino acids shorter than the known full-length transcript. Quantitative PCR (qPCR) confirmed that Tsacc is expressed in skeletal muscle with expression increasing as muscle cells undergo differentiation. Characterization of Tsacc transcriptional activity revealed that Tsacc gene activity is modulated by myogenic regulatory factors (MRFs) and is significantly induced by MyoD. Moreover, sub-cellular localization was assessed by confocal microscopy, which showed that the two Tsacc proteins produced by the two alternatively spliced transcripts had distinct localization patterns. Tsacc-FL localized exclusively to the cytoplasm of muscle cells while Tsacc-novel localized diffusely within the cell, appearing in both the nucleus and cytoplasm of muscle cells. Finally, Western blot analysis revealed that ectopic expression of the full-length Tsacc transcript in C_2C_{12} resulted in significant inhibition of conical markers of muscle differentiation, including MyHC and myogenin while the novel Tsacc transcript did not. The impact of Tsacc on the AKT signaling pathway, which is known to participate in the regulation of muscle size, was also assessed. Overexpression of either the full-length or novel Tsacc transcript was found to modulate the AKT signaling pathway in cultured muscle cells. Understanding the role of Tsacc will further our understanding of the molecular and genetic mechanisms of the muscle wasting and potentially provide new therapeutic targets for mitigating the negative outcomes associated with muscle atrophy.

Part I: Introduction and Background

Skeletal muscle and skeletal muscle atrophy

Skeletal muscle is a dynamic tissue that has the ability to respond to physiological and pathophysiological stimuli by differential regulation of protein synthesis and protein turnover pathways. An imbalance between protein synthesis and protein degradation can lead to abnormal muscle mass resulting in gain or loss of muscle mass. These two conditions are known as hypertrophy and atrophy, respectively. Physical activity such as resistance training can lead to muscle hypertrophy while conditions such as cachexia, inflammation, aging, and increased corticosteroid levels can all lead to muscle atrophy.

Muscle atrophy is defined as the reduction in muscle mass and contractile strength. Proteolysis, the breakdown of proteins, is an essential process for cell survival allowing the body to get rid of damaged, defective, or unneeded proteins. Yet when protein degradation outweighs protein synthesis, a decrease in muscle mass occurs (Egerman and Glass, 2014). Two main proteolytic systems that control this protein turnover in cells are the ubiquitin proteasome system (UPS) and the autophagy lysosome system (ALS).

The Ubiquitin Proteasome System (UPS)

The ubiquitin proteasome system (UPS) utilizes three enzymes that function in conjunction with the 26S proteasome. These three enzymes are known as the E1 ubiquitin-activating enzyme, the E2 ubiquitin-conjugating enzyme, and the E3 ubiquitin ligase. The UPS pathway is initiated by the activation of a 76-amino acid ubiquitin protein by an E1 enzyme, leading to the formation of a thioester bond between the carboxyl terminus of ubiquitin and the cysteine of the active site on the E1 (Fig. 1). The activated ubiquitin is then transferred to the E2 enzyme, which is then ligated to the target substrate to tag it for degradation (McKinnell, 2004). The transfer of ubiquitin

is achieved when the E3 ligase simultaneously binds with an E2 and a specific target substrate (McKinnell, 2004). Therefore, the E3 ligase is generally believed to provide the selectivity and specificity of the many different targets of the UPS pathway. To promote substrate turnover, the conjugation and ubiquitin transfer cycles continue until the substrate accumulates four or more molecules of ubiquitin, which then triggers degradation by the 26s proteasome (Fig. 1).

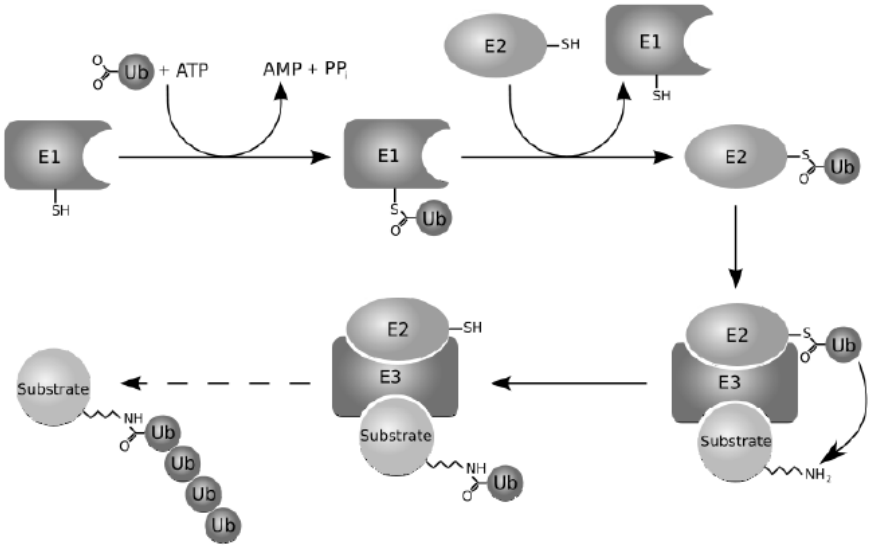

Figure 1: Schematic of the ubiquitin proteasome system. The E1 ubiquitin activating enzyme, E2 ubiquitin conjugating enzyme, and E3 ubiquitin ligase form a pathway to ubiquitinate substrates for degradation by the 26s proteasome (Adapted from Egerman, 2014).

Differential Gene Expression in Response to Denervation-induced Atrophy

Because the specificity of protein degradation is dictated by the E3 ubiquitin ligases, identification of E3 ubiquitin ligases is of importance to better understand the muscle atrophy pathway. To identify potential atrophy promoting genes, Bodine et al. subjected rats to different atrophy stimuli including denervation, immobilization, and hind limb suspension. Interestingly, two genes that encode for ubiquitin E3 ligases were found to be upregulated in all three models of atrophy and were named Muscle RING Finger 1 (MuRF1) and Muscle Atrophy F-box (MAFbx) (Fig.2). To further evaluate the function of these two genes, MAFbx and MuRF1 knockout (KO)

mice were generated through β-galactosidase lacZ cassette insertion into the genomic region of each gene. MAFbx-null and MuRF1-null mice were then subjected to denervation of the tibialis and gastrocnemius muscles for 14 days and compared to wild-type mice. The MuRF1-null mice showed 36% muscle sparing while the MAFbx-null mice showed 56% muscle sparing (Bodine et al., 2001). Even though the MAFbx knockouts showed a greater percentage of muscle sparing, the MuRF1 knockouts displayed greater muscle integrity, making MuRF1 the leading candidate for therapeutic intervention of muscle atrophy (Furlow et al., 2013).

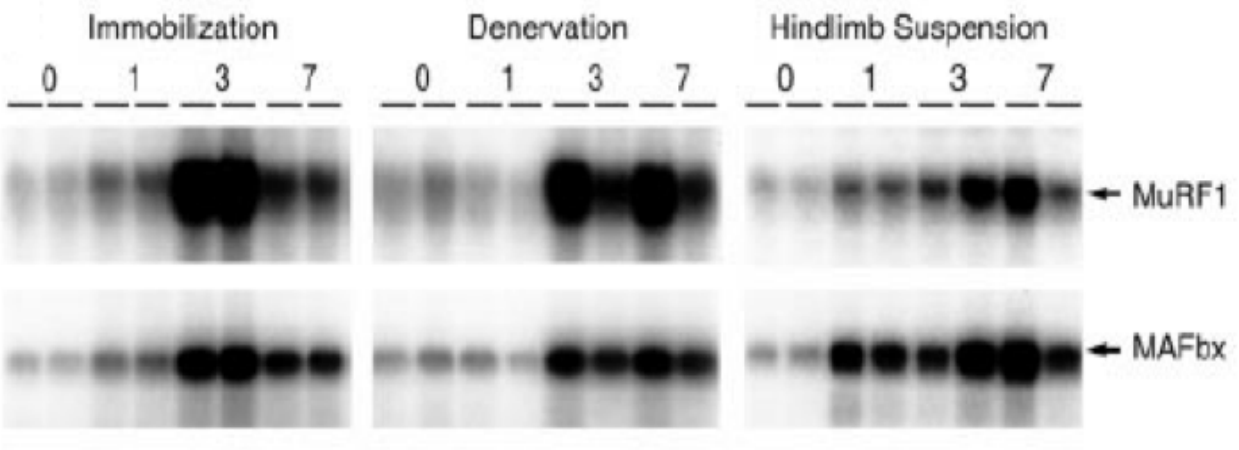

Figure 2. MuRF1 and MAFbx are upregulated during muscle atrophy. Northern blot displaying mRNA expression of MuRF1 and MAFbx in muscle tissue of rats subjected to atrophy induction by immobilization, denervation, and hind limb suspension. Increased expression is observed at day 1 and reaches a peak at day 3 post-denervation (Bodine et al, 2001).

MuRF1 is a member of the TRIM family, which is composed of about 80 E3 ubiquitin ligases that are characterized by a RING domain, a zinc-finger B-box domain, and a leucine-rich coiled-coil domain (Bodine and Baher, 2014). The RING domain of E3 ubiquitin ligases has a role in bringing the substrate protein and ubiquitin from the E2 into contact. The RING domain, which consists of important cysteine and histidine residues is believed to perform the catalytic activity of MuRF1, while the zinc-finger B-box domain is suggested to function in binding to DNA or other

proteins (Ikeda and Inoue, 2013). While it is clear that MurF1 plays an important role in the skeletal muscle atrophy, the exact molecular function of this E3 ligase is not well understood and very few validated targets have been identified (Bodine and Baehr, 2014). Moreover, the lack of clearly identified protein targets has led to further evaluation of MuRF1's specific role in skeletal muscle atrophy.

To better understand MuRF1's role in skeletal muscle, Furlow et al.,2013 conducted a genome-wide transcriptomic analysis comparing MuRF1 knockout (KO) mice with wild-type (WT) mice following denervation for 3 and 14 days. The goal of the microarray study was to identify genes that are differentially regulated in WT mice compared to atrophy resistant MuRF1-KO mice. The MuRF1-null mice were generated by insertion of a β-gal-encoding lacZ cassette into the MuRF1 gene locus insertion to disrupt the MuRF1 gene and introduce β-galactosidase when the MuRF1 promoter is active, allowing for assessment of endogenous MuRF1 promoter activity without the effect of the functional MuRF1 gene. Gastrocnemius muscle tissue was isolated at 3- and 14-days post-denervation and a genome wide microarray was conducted (Furlow et al., 2013). In order to confirm knockout, MuRF1 expression in MuRF1 KO mice was evaluated and found to be missing as expected. In contrast, the WT mice displayed an increase in expression of MuRF1 at 3 days post-denervation that returned to baseline by 14 days post-denervation (Fig 3A). Interestingly, in the KO mice β-galactosidase expression was elevated at day 3 post-denervation and remained elevated at day 14 post-denervation, suggesting that MuRF1 might be negatively regulating its own expression (Fig 3B).

MAFbx expression was also evaluated in the WT mice in response to denervation and was found to have increased expression at day 3 post-denervation and a return to baseline by day 14 (Fig 3C). However, in the MuRF1 KO mice, MAFbx expression was elevated at day 3 post-

denervation and remained elevated at day 14 post-denervation, suggesting that MuRF1 may not only be negatively regulating itself but also negatively regulating MAFbx expression (Fig 3D).

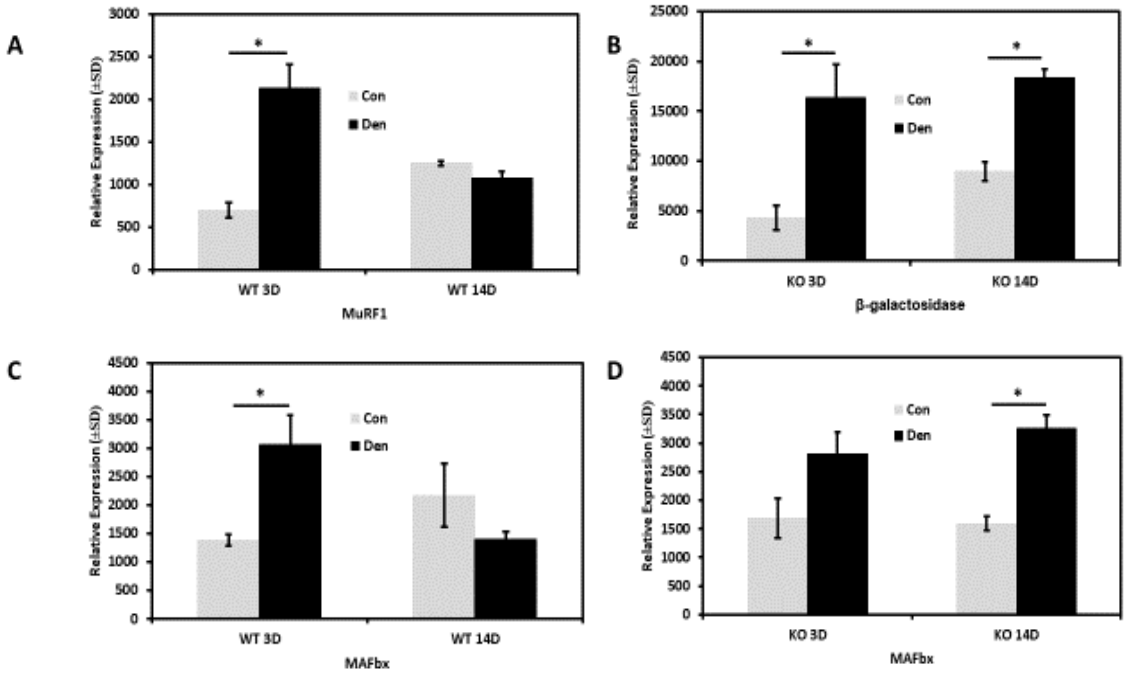

Figure 3. Transcriptional activity of the MuRF1 gene locus and MAFbx in WT and MuRF1 KO mice post-denervation. (A) Denervated WT mice show an increase in MuRF1 gene expression at day 3 (3D) but returns to baseline at day 14 (14D) post-denervation. (B) Denervated KO mice show an increase in β-galactosidase expression, which is under the control of the MuRF1 promoter, at day 3 and expression remained elevated at day 14 post-denervation. (C) Denervated WT mice show an increase in MAFbx gene expression at day 3 (3D) but a return to baseline levels by day 14 (14D) post-denervation. (D) Denervated MuRF1 KO mice showed increased expression in MAFbx at day 3 (3D) that remained elevated at day 14 (14D) (Furlow et al, 2013).

Moreover, beyond MuRF1 and MAFbx, our lab has also identified and characterized a number of other differentially expressed genes in MuRF1-null mice in response to denervation, including Ttc389, Dusp4, Dupd1/Dusp29, Fam83d, and Zfp593 (Hayes et al, 2019, Haddock et al, 2019, Cooper et al, 2020a, Cooper et al, 2020b, Lynch et al, 2019). In addition to genes differentially expressed in MuRF1-null mice, the microarray study also identified hundreds of genes that were differentially expressed in mice undergoing neurogenic atrophy regardless of genotype. Many of these differentially expressed genes exhibited a range of different functions,

with some known to play a role in muscle structure and function, while others have been linked to metabolic pathways and signal transduction cascades. Importantly, a subset of genes induced in response to denervation have not been previously characterized in skeletal muscle or any other tissue, including TSSK6 Activating Co-chaperone (TSACC), which is the focus of this study.

Myogenic regulatory factors (MRFs) are upregulated during muscle differentiation and atrophy

Myogenesis, the process of muscle cell development is controlled through myogenic regulatory factors (MRFs). MRFs are a family of muscle specific factors that control both pre-natal and post-natal myogenesis. During embryonic development, mesodermal cells generate myogenic cells that ultimately give rise to differentiated skeletal muscle tissue. Yet, a subset of these myogenic cells form satellite cells instead. These satellite cells acts as adult stem cells and are responsible for muscle regeneration and development after birth. Upon injury, satellite cells begin to proliferate and divide into myoblasts and then differentiate into myotubes, giving rise to mature muscle tissue (Fig. 4). MRFs regulate this highly orchestrated process and function by interacting with co-activators and co-repressors at the promoter regions of muscle-specific genes. (Hettmer and Wagers, 2010). The structure of MRFs is characterized by the presence of a basic helix-loop-helix domain (bHLH) that allows binding with E-box consensus sequences (5'-CANNTG-3') located within the promoters of many muscle-specific genes.

MyoD and myogenin are two MRFs that have been shown to be upregulated during neurogenic atrophy (Furlow et al, 2013). MyoD acts as a marker of myogenic commitment to skeletal muscle and plays a role in early myogenesis by promoting myoblast proliferation, while myogenin plays a key role in late myogenesis, promoting muscle cell differentiation and the fusion of myoblast into myotubes (Hindi et al, 2017). Additionally, myogenin is essential for full induction of MuRF1 and MAFbx under neurogenic atrophy conditions and previous studies have shown that the

deletion of myogenin leads to lower levels of MuRF1 and MAFbx expression and resistance to muscle wasting in mice subjected to denervation (Dilworth, Singh, 2013).

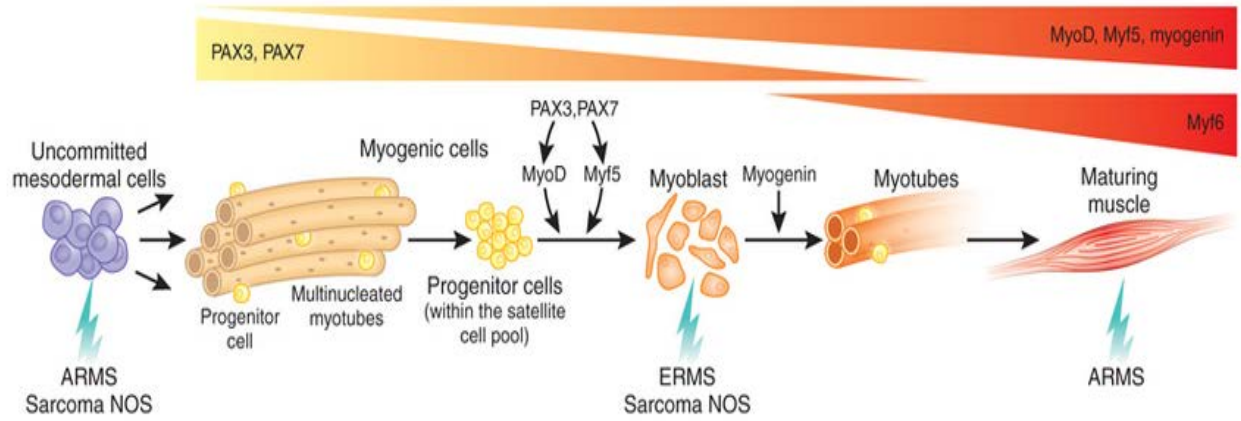

Figure 4. Process of muscle cell development is controlled by myogenic regulatory factors (MRFs). MyoD and myogenin are two MRFs that play a critical role in muscle cell proliferation and differentiation, respectively (Hettmer and Wagers, 2010)

Mitogen-activated protein kinase (MAPK) signaling

Mitogen-activated protein kinase (MAPK) signaling plays a critical role in growth and repair of muscle tissue upon injury. It has been shown that MAPK signaling is important for muscle cell differentiation, specifically complete differentiation, and fusion of myoblasts into myotubes (Bennett and Tonks, 1997). MAPK signaling involves four pathways including extracellular signal-related kinase 1/2 (ERK1/2), p38, c-Jun N-terminal kinase (JNK), and ERK5, which have all been implicated in muscle cell proliferation, migration, differentiation, and fusion (Fig. 5). The ERK1/2 signaling pathway is active during myoblast proliferation, decreases as cells differentiate and then peaks again at terminal differentiation to induce myoblast fusion into myotubes (Bennett and Tonk, 1997). The p38 branch is activated during muscle cell differentiation and is required for myotube formation, while JNK signaling negatively regulates muscle cell differentiation and is downregulated in late myogenesis (Xie et al., 2018). ERK5 has been implicated in stimulation of myoblast fusion and when blocked, myoblast fusion and the formation of multinucleated myotubes

is inhibited (Hindi et al., 2013). These pathways are highly regulated and may function concurrently during muscle development and repair following injury (Hindi et al., 2013).

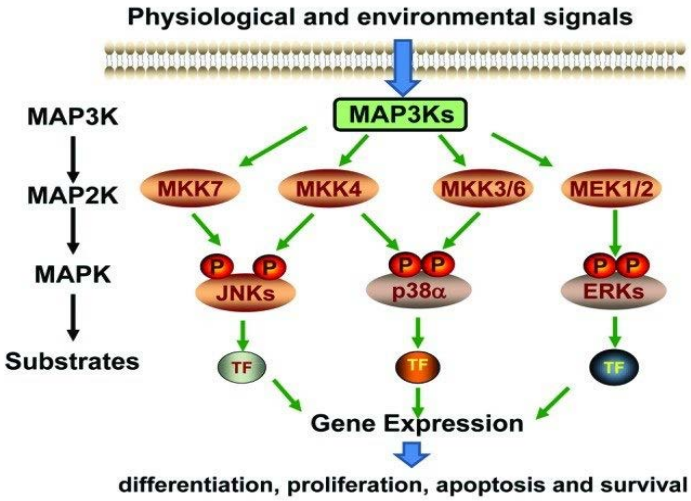

Figure 5. Schematic of the MAPK signaling pathways (Wang and Xia, 2012).

AKT signaling cascade

MAPK is not the only signaling pathway involved in muscle growth and myogenesis. The serine/threonine kinase AKT/protein kinase B is activated by insulin-like growth factor (IGF) and functions to activate the expression of proteins related to protein synthesis, such as mTOR. Moreover, activated AKT suppresses the activity of the FoxO family of transcription factors, which are known to promote skeletal muscle atrophy. Thus, AKT is essential in regulating both protein synthesis as well as protein degradation pathways, which work in tandem to regulate muscle mass (Egerman and Glass, 2014) (Fig.6).

AKT has been found to stimulate protein synthesis via two branches. The first branch is through the activation of mTOR. The activation of mTOR leads to the phosphorylation of its downstream target 4E-BP1. Phosphorylated 4E-BP1 is then no longer able to bind and inhibit the eIF4E initiation factor that is essential for protein translation, which leads to an increase in protein

translation levels within muscle cells. The second mechanism is through AKT phosphorylation of Glycogen synthase kinase 3β (GSK-3β). GSK-3β is constitutively active and functions by inhibiting protein synthesis (Schiaffino and Mammucari, 2011). The phosphorylation of GSK-3β leads to its inactivation and inability to phosphorylate and inhibit downstream protein targets related to protein synthesis.

AKT inhibits protein degradation by phosphorylating and repressing transcription factors of the FoxO family, which are required for transcriptional regulation of the E3 ubiquitin ligases MuRF1 and MAFbx (Stitt et al., 2004). Thus, AKT indirectly results in the inhibition of the transcriptional activity of both MuRF1 and MAFbx. Due to the role of AKT in regulating identified mediators of skeletal muscle cell function, genes that potentially regulate the activation of AKT are of interest for elucidating the mechanisms by which the atrophy cascade proceeds.

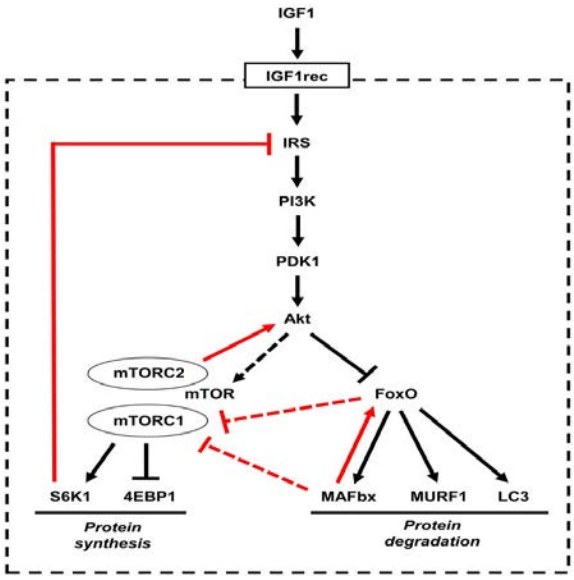

Figure 6. The insulin-like growth factor 1(IGF1)-Akt pathway controls muscle growth via mammalian target of rapamycin (mTOR) and FoxO proteins. (Schiaffino and Mammucari, 2011).

Identification and characterization of TSSK6 Activating Co-chaperone (TSACC) in skeletal muscle

Overview

TSSK6 Activating Co-chaperone (Tsacc) is a protein coding gene that is exclusively found in mammals. Previous studies have shown that Tsacc plays an important role as a co-chaperone by binding to HSP70 and facilitating HSP90 mediated TSSK6 activation (Jha et al., 2010). TSKK6 activation appears to be necessary for male fertility in mammals and it has been shown that the male infertility phenotype has been associated with a mutation or absence of the Tsacc gene in maturing spermatids (Jha et al., 2017). Even though most studies are concerned with Tsacc's role on spermatogenesis, one study found that Tsacc may also play an important role in regulating cell proliferation, apoptosis, and differentiation (Capra, 2006). While there is some data on the putative functions of Tsacc, the exact role of this gene in skeletal muscle has not been previously investigated. Therefore, the goal of this study was to characterize and elucidate the potential function of Tsacc in skeletal muscle.

Materials and Methods

Animals

There were no animal experiments related to the current study conducted at the University of North Florida; however, the sex, age range, strain, and treatment conditions of the animals used for the Illumina microarray studies, as well as the IUCAC approvals, have been previously described (Furlow et al., 2013)

Cell Culture

C_2C_{12} mouse myoblasts were maintained in Dulbecco's Modified Eagle's Medium (DMEM) (Thermo Fischer Scientific, Waltham, MA) supplemented with 10% Fetal Bovine Serum (FBS) (GE Healthcare HyClone Laboratories, Logan, UT), 1X Penicillin/Streptomycin and Gentamicin

(Thermo Fischer Scientific, Waltham, MA), and non-essential amino acids (GE Healthcare HyClone Laboratories, Logan, UT). Cells were maintained in a humidified chamber at 37°C and 5% CO_2. Cells were grown to 100% confluency and switched to DMEM supplemented with 2% serum to induce differentiation.

RNA isolation and complementary DNA synthesis

Total RNA was isolated from C_2C_{12} myoblasts and myotubes using the RNeasy Mini Kit (Qiagen, Valencia, CA) following the manufacturer's instructions. Isolated RNA was used to synthesize complementary DNA (cDNA) using a PolyT primer and Moloney Murine Leukemia Virus (M-MLV) Reverse Transcriptase according to the manufacturer's instructions (Thermo Fisher Scientific, Waltham, MA).

Amplification and cloning of the Tsacc cDNA

For the amplification of the Tsacc cDNA, gene-specific primer pairs were designed (Table 1) using the gene sequence for murine Tsacc (GenBank accession number: NM_029801.2) and mixed with template DNA generated by reverse transcription described above according to the manufacturer's recommendation (ThermoFisher Scientific, Waltham, MA). Tsacc cDNA was subcloned into the EcoRI and XbaI sites of the pcDNA3 (+) (ThermoFisher Scientific, Waltham, MA) and pCS2(+)-myc expression plasmids. The cDNA of Tsacc was also fused in frame with GFP by cloning into the EcoRI and XbaI sites of the pEGFP-C1 expression plasmid (Clontech, Mountain View, CA).

Table 1. Primer Sequences Used in This Study

Primer Name	Primer Sequence (5' to 3')
Tsacc-cDNA-F	GCGAATTCCAAGATGGAGCAGCACACTAGTAACC
Tsacc-cDNA-R	GCTCTAGACAGCTCATTTATGGAATTGGGGCAGG
Tsacc-qPCR-F1	GAAGCTCTGTTTTGTCCATCGG
Tsacc-qPCR-R1	GTAGGGTTACTAGTGTGCTGC
Tsacc-qPCR-F2	CTTGACCATCCAGACAAAGC
Tsacc-qPCR-R2	CTATCTGTCGTTGAGCAAGC
Tsacc-qPCR-F3	TCTTCAGGAGCTGGTCAGAAG
Tsacc-Pro1000-F	GCACGCGTGTGCTCTTTACTGAGATGAGTGGCG
Tsacc-Pro500-F	GCACGCGTGAGCTTGGTCCAAGGCGAAAAGACC
Tsacc-Pro-R	GCGAATTCCCTACAGCATTAATCCAAAGCCTCC

Promoter cloning of the TSACC gene

For the amplification of the regulatory region of Tsacc, genomic DNA was isolated from C_2C_{12} cells using the DNeasy Blood and Tissue Kit (Qiagen, Valencia, CA) according to the manufacturer's protocol. PCR was preformed using Tsacc promoter region-specific primer pairs (Table 1) generated using mouse genomic sequences obtained from the Ensembl database (www.ensembl.org). PCR was performed using the manufacturer's protocol (Life Technologies, Grand Island, NY). PCR products were then ligated into the pGEMT-EZ vector (Promega, Madison, WI) according to the manufacturer's protocol and sequenced to confirm amplification of the predicted target region. Tsacc promoter fragments (~500 and ~1000 base pairs) were sub-

cloned into the EcoRI and MluI sites of the pSEAP2-Basic reporter plasmid (Clontech, Mountain View, CA) to create the pSEAP-Tsacc-Pro500 and pSEAP-Tsacc-Pro1000 reporter plasmids and sequenced to confirm correct orientation.

Reporter Assays

C_2C_{12} myoblast cells were plated in 12-well plates at approximately 75,000 cells/well and cultured overnight. Cells were transfected at 70-80% confluency using Turbofect Transfection Reagent (Thermo Scientific, Rockford, IL) and following manufacturer's protocol. Briefly, a total of 1µg per well of DNA (250ng/well reporter plasmid, 125ng/well of β-galactosidase (β-gal) and empty pBluescript vector as filler DNA) was mixed with transfection reagent and allowed to complex for 20 minutes prior to overlaying the cells. Following transfection, cells were incubated for 24 hours, and culture media was then changed from DMEM + 10% serum to DMEM + 2% serum to induce differentiation. Growth media was collected at 24-72 hours after the switch to differentiation media and tested for SEAP levels using the Phospha-Light SEAP Reporter Gene Assay Kit and following the manufacturer's instructions (Life Technologies, Grand Island, NY). The level of SEAP generated luminescence was assessed using a BioTec Synergy 2 microplate reader set for an endpoint read with a 2 second integration time. To account for any variation in transfection efficiency, cells were lysed using Passive Lysis Buffer (Promega, Madison, WI) and were cleared of cell debris by centrifugation. Cell lysates were incubated with ortho-nitrophenyl-β-D-galactopyranoside (ONPG) dissolved in Z Buffer (60mM Na2HPO4·7H2O, 40mM NaH2PO4·H2O, 10mM KCl, 1mM MgSO4, 50mM β-mercaptoethanol, pH 7.0) overnight at 37°C. Following overnight incubation, β -gal activity was analyzed and used to correct the SEAP values.

Bioinformatic analysis of Tsacc

DNA sequences corresponding to the promoter regions of human, rat, and mouse Tsacc (EnsemblTranscriptID:ENSG00000163467,ENSRNOG00000037552,andENSMUSG00000010538, respectively) starting at -2000 and including the first exon were taken from the Ensembl database (www.ensembl.org) and analyzed using the Clustal Omega multiple sequence alignment tool available on the EMBL-EBI website (https://www.ebi.ac.uk/Tools/msa/clustalo/). The Clustal Omega alignment data was then analyzed using Boxshade version 3.21 (http://www.ch.embnet.org/software/BOX_form.html) that is available on the ExPASy (www.expasy.org) website. The polypeptide sequences for human, mouse, and rat Tsacc were also downloaded from Ensembl and aligned using the Clustal Omega alignment tool and shaded with Boxshade as described for the promoter sequences above.

Reverse transcription quantitative PCR (RT-qPCR)

Total RNA was isolated from proliferating and differentiating C_2C_{12} cells (as described above) and reverse transcribed using the iScript cDNA synthesis kit according to manufacturer's protocol (Bio-Rad, Hercules, CA). The resulting cDNA was mixed with gene specific primers (Table 1) and iTaq Universal SYBR Green Reaction Supermix according to manufacturer's instruction and Tsacc gene expression was then analyzed using a CFX connect Real-Time PCR Detection System (Bio-Rad, Hercules, CA). Gene expression was analyzed at varying timepoints, each timepoint was performed in biological triplicate, each individual biological replicate was used for cDNA amplification in duplicate, and each cDNA amplification replicate was done in technical triplicates (three biological replicates × two cDNA synthesis replicates × three technical replicates = 18 individual reads per biological sample). Relative gene expression was calculated using the $2^{-\Delta\Delta Ct}$ method and GAPDH as the reference gene.

Protein purification and Western blot analysis

C_2C_{12} cells were cultured in 10 cm culture plates and Tsacc was exogenously expressed by transfecting cells with the pCS2(+)-myc-Tsacc full-length (FL) and novel expression plasmids 24 hours post plating. Transfection mix was prepared as previously described above. Cells were harvested at cell proliferation (DMEM + 10% serum) day 2 and differentiation (DMEM + 2% serum) days 1, 3, and 5 (PD2, DD1, DD3, and DD5) and stored at -80 C until cell lysis and protein purification were performed.

Harvested cells were lysed on ice in Universal Lysis Buffer $(ULB)^{(+)}$ (50mM Tris, pH 7.5, 150mM NaCl, 50mM NaF, 0.5% NP-40, with addition of 1mM PMSF, 1mM DTT, 10mM β-glycerophosphate, 2mM sodium molbydate and a protease inhibitor cocktail). Cell debris was cleared through centrifugation and protein concentration was determined using the Quick Start Bradford 1x Dye reagent following the manufacturer's instruction (Bio-Rad, Hercules, CA).

Western blots were conducted using 25-100μg of protein separated on a 10% sodium dodecyl sulfate polyacrylamide gel electrophoresis (SDS-PAGE) denaturing gel and then transferring to polyvinylidene fluoride (PVDF) membrane (EMD Millipore, Billerica, MA) overnight. Quality of the transfer and equal protein loading was verified by Ponceau S staining of the membranes. Following staining, membranes were blocked using a blocking solution composed of 5% dry milk dissolved in Tris-buffered saline and 0.05% Tween-20 (TTBS). Westerns blots were probed with 5% dry milk dissolved in Tris-buffered saline and 0.05% Tween-20 (TTBS). The membranes were probed with anti-myosin heavy chain (MYH1/2/4/6), anti-myogenin, anti-p-ERK, anti-ERK, anti-AKT-phospho-S473, anti-AKT, anti-GAPDH, and anti-myc primary antibodies and subsequently probed with a corresponding species specific HRP-conjugated secondary antibody (Table 2). Westerns were visualized using ECL Western Blotting Substrate (Thermo Fisher Scientific, Waltham, MA) following manufacturer's protocol and imaged using an Amersham Imager 600

RGB system (GE Healthcare Life Sciences, Marlborough, MA). PVDF membranes were stripped by incubating the membrane in stripping buffer (10% SDS, 0.5M Tris-HCl pH 6.8, β-mercaptoethanol solution) for 20-30 mins and then blocked again, re-probed, and imaged as described previously.

Table 2. List of antibodies used in this study

Antibody	**Source**	**Catalog #**	**Dilution**
anti-myc	ProteinTech, Rosemont, IL	600032-1g	WB: 1:1000
anti-Myosin Heavy Chain (MYH1/2/4/6)	Santa Cruz Biotechnology, Dallas, TX	sc-32732	WB: 1:1000
anti-myogenin	Santa Cruz Biotechnology, Dallas, TX	sc-12732	WB: 1:1000
anti-GAPDH	ProteinTech, Rosemont, IL	600041-lg	WB: 1:5000
anti-phospho-ERK1/2	Santa Cruz Biotechnology, Dallas, TX	sc-7383	WB: 1:1000
anti-ERK1/2	Santa Cruz Biotechnology, Dallas, TX	sc-94	WB: 1:1000
anti-AKT-phospho-S473	ProteinTech, Rosemont, IL	66444-I-lg	WB: 1:2000
anti-AKT	ProteinTech, Rosemont, IL	602032-lg	WB: 1:5000
Mouse anti-rabbit IgG-HRP	Santa Cruz Biotechnology, Dallas, TX	sc-2357	WB: 1:5000
Rabbit anti-mouse IgG-HRP (H + L)	Thermo Scientific, Rockford, IL	PI31450	WB: 1:5000

Confocal fluorescent microscopy

C_2C_{12} cells were plated on 3.5cm glass bottom plates at a density of 100,000 cells/plate and transfected with either 2.5µg pEGFP-Tsacc or empty pEGFP plasmid using Turbofect transfection reagent at 70-80% cell confluency. At 48 hours post-plating, cells were fixed with 4% paraformaldehyde dissolved in 0.1 M Sodium Cacodylate and stained with DRAQ5 nuclear stain (ThermoFisher Scientific, Waltham, MA). Imaging was conducted on an Olympus Fluoview FV-1000 confocal fluorescent microscope with a Super Apochromat UPLSAPO 20X objective or a Super Apochromat UPLSAPO 60X objective. The GFP and DRAQ5 images were then merged using the open access ImageJ software and utilizing the Open Microscopy Environment Bio-Formats software plugin tool.

Statistics

Data are presented as the mean ± standard deviation (±SD). Statistical analysis was conducted using a two-tailed *t*-test and a difference was considered statistically significant at a P value ≤ 0.05.

Results

Tsacc is induced during neurogenic atrophy.

To better characterize the molecular genetic events of neurogenic atrophy, mouse gastrocnemius muscle was isolated following 3 days and 14 days of sciatic nerve denervation. The gene expression profile was analyzed through an Illumina mouse-6 v1.1 expression beadchip array, as previously described (Furlow et al., 2013). Results from the microarray identified a significant number of genes that were differentially expressed in response to neurogenic atrophy. Many of these genes were novel and have not been previously implicated in atrophy or characterized in skeletal muscle, with Tsacc being among these novel genes. Microarray analysis revealed that Tsacc is expressed at relatively low levels in control muscle tissue and is significantly

induced in response to neurogenic atrophy 14 days post-denervation (Fig 7A and 7B). Additionally, the microarray examined if MuRF1 expression had an effect on Tsacc expression. Both MuRF1-null mice and wild-type mice displayed relatively similar Tsacc expression profiles at both 3 days and 14 days post-denervation (Fig 7A and 7B).

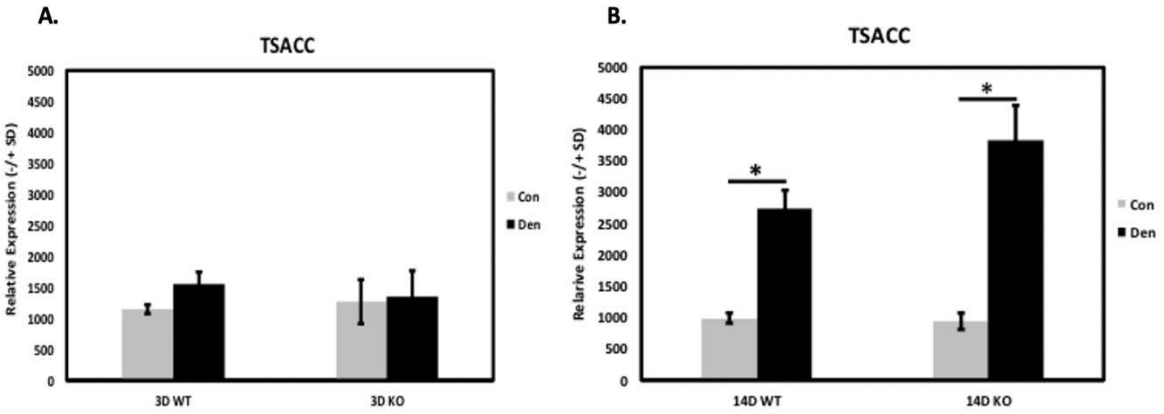

Figure 7. Tsacc is induced in response to denervation-induced skeletal muscle atrophy. Whole genome expression analysis was conducted on triceps surae muscle from wild-type (WT) and MuRF1-null (KO) control mice after 3 days (3D) and 14 days (14D) post-denervation (DEN). Tsacc expression was unchanged in WT and KO mice at (**A**) 3 days post-denervation, but increased significantly at (**B**) 14 days post-denervation in the wild-type and MuRF1-null animals. Each condition represents the average expression from three animals and error bars represent ± SD. Grey bars represent the controls (Con) and black bars represent denervation (Den). Significant difference between denervated mice and control mice in the same group (*:$P < 0.01$).

Tsacc expression is regulated by Myogenic Regulatory Factors

To gain insight into how Tsacc is regulated transcriptionally in muscle cells, 500 and 1000 base pairs of the promoter were amplified using the primers listed in Table 1. The fragments were then fused to a secreted alkaline phosphatase (SEAP) reporter gene to create the pSEAP-Tsacc-Pro500 and pSEAP-Tsacc-Pro1000 reporter constructs. The Tsacc reporter gene constructs were transfected into C_2C_{12} mouse myoblasts and SEAP assays were performed 48h after the switch to differentiation media. Both promoter fragments showed higher expression compared to the empty plasmid alone (Fig. 8A and 8B). To further analyze the transcriptional activity of Tsacc, cells were co-transfected with a MyoD expression plasmid along with the Tsacc reporter gene constructs. MyoD, a myogenic regulatory factor (MRF), is a known transcription factor that is muscle specific and has a role in myogenesis. Overexpression of MyoD significantly induced the transcriptional activity of both the pSEAP-Tsacc-Pro500 and pSEAP-Tsacc-Pro1000 reporter constructs (Fig. 8A and 8B). Importantly, bioinformatic analysis of the promoter region of Tsacc revealed four predicted MyoD binding sites within the first 500 bps upstream of the start of transcription (Fig 8C).

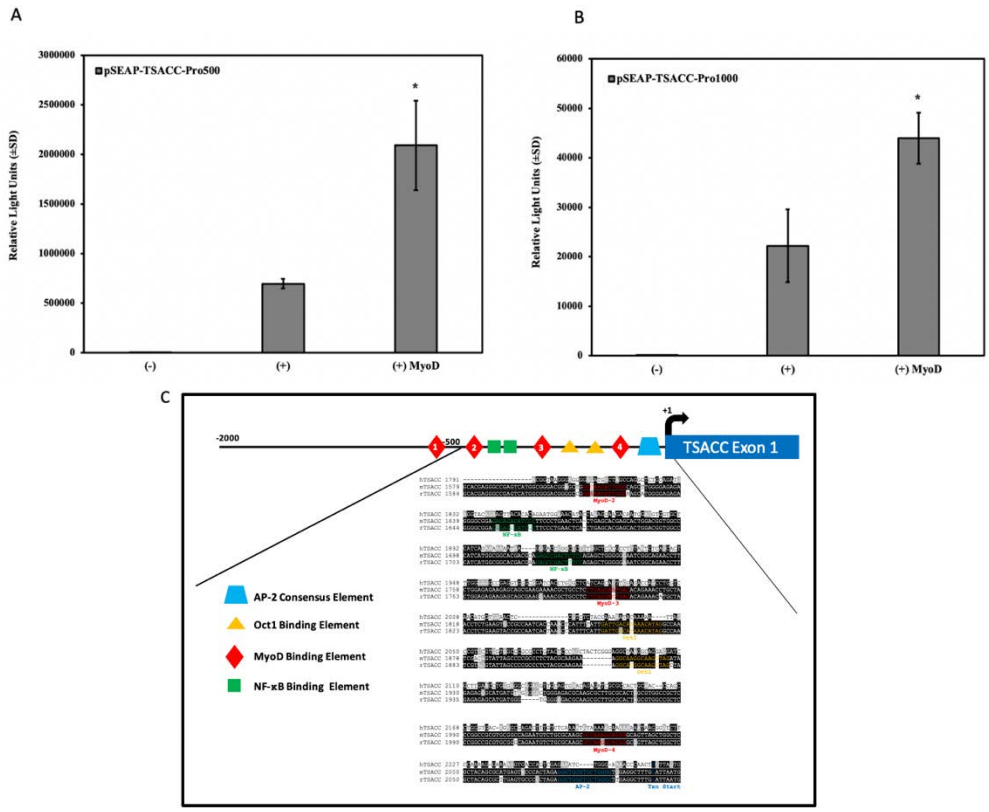

Figure 8. Cloning and analysis of the proximal regulatory region of the Tsacc gene locus. Secreted Alkaline Phosphatase (SEAP) reporter gene analysis of culture media from C_2C_{12} cells transfected with either the (A) pSEAP-Tsacc-Pro500 or the (B) pSEAP-Tsacc-Pro1000 reporter constructs with or without a MyoD expression plasmid. The empty pSEAP vector served as a negative control. The culture media was changed to low serum media 24 hours post-transfection to induce differentiation and the culture media was then sampled 48 hours post-media change. The SEAP numbers were normalized to β-galactosidase activity to correct for variations in transfection efficiency. Each condition was performed in triplicate and each experiment was repeated at least three times (n=3). The graphs are of a representative experiment and values correspond to the mean relative light unit (RLU) values ± SD. Significant differences between the activities of the pSEAP2-Tsacc-Pro reporter constructs with and without MyoD ectopic expression (* = $P \leq 0.05$). (C) Schematic and sequence alignment of the Tsacc regulatory region. Promoter sequences from mouse, rat, and human Tsacc (2000 base pairs upstream of the transcription site (+1) through the first exon) were downloaded from the Ensembl database (www.ensembl.org) and aligned using the ClustalW algorithm. Regions highlighted in black show identical sequences between the three species. Approximate positions of potential transcription factor binding sites are highlighted in the alignment: AP-2 Consensus Binding Element (blue trapezoid); Oct1 Binding Element (yellow triangle); MyoD Binding Element (red diamond); NF-κB Consensus Binding Element (green square).

Tsacc is alternatively spliced in muscle cells

To better characterize the role of Tsacc in skeletal muscle, cloning of the Tsacc gene from cultured muscle cells resulted in the identification of a novel transcript of Tsacc. The novel Tsacc transcript contains an extra exon compared to the full-length transcript of Tsacc (Fig. 9), giving rise to a protein that is different in size. The novel Tsacc protein is predicted to be 49 amino acids shorter than the FL Tsacc protein as a result of the extra exon (Fig. 9).

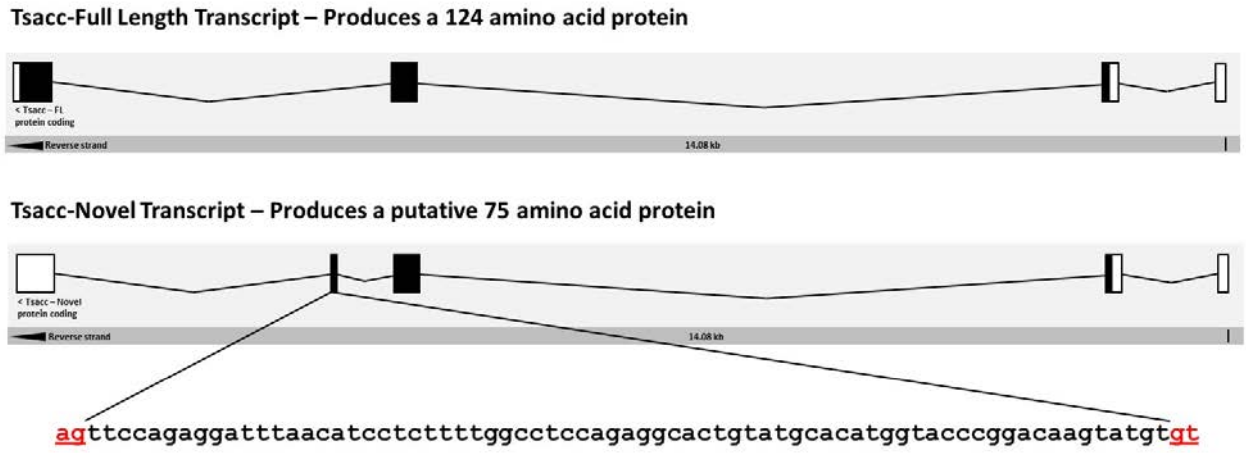

Figure 9. Schematic of the validated Tsacc transcript and a newly discovered Tsacc novel transcript. The boxes represent exons, and the connecting lines represent introns. An extra exon which produces a shorter 75 amino acid protein is observed in the novel Tsacc transcript compared to the full-length transcript. This expanded exon region contains classic intron and exon boundaries which are highlighted in red.

Tsacc is upregulated during muscle cell differentiation

To analyze the transcriptional expression of Tsacc during muscle cell differentiation. C_2C_{12} cells were cultured, differentiated, and harvested over a time course of proliferation day 2 (PD2), differentiation day 2 (DD2), and differentiation day 7 (DD7). RNA was isolated and used for analysis of Tsacc expression by reverse transcription quantitative polymerase chain reaction (RT-qPCR). Three primer pairs spanning different regions of the Tsacc gene were used. Primer pair one spanned through the 5' untranslated region (5'-UTR), primer pair two spanned across the exon

2 and exon 3 boundary, and primer pair three spanned across the exon 2 and exon 4 boundaries (Table 1). The qPCR analysis confirmed that Tsacc is expressed in muscle cells and increases as cells differentiate, with the lowest expression during proliferation and highest expression during late differentiation (Fig. 10).

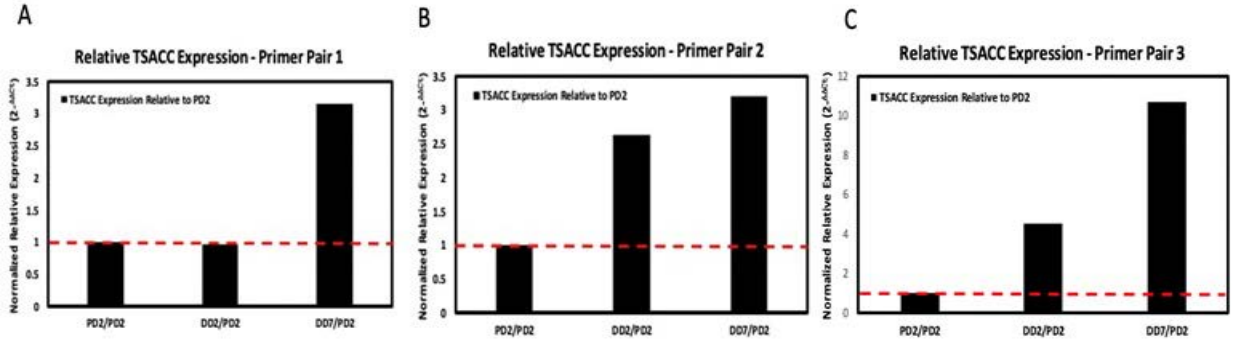

Figure 10. qPCR analysis of Tsacc expression in C_2C_{12} cells. Three primer pairs spanning three different regions of the Tsacc mRNA were used for qPCR. RNA was extracted from C_2C_{12} cells at proliferation day 2 (PD2), differentiation day 2 (DD2), and differentiation day 7 (DD7). cDNA samples were subsequently analyzed by qPCR and normalized in comparison to PD2. For primer pairs 1 **(A)**, 2 **(B)**, & 3 **(C)**, the relative expression of Tsacc was found to increase from PD2 to DD7 in C_2C_{12} cells. Relative expression of Tsacc was normalized to GAPDH expression using the $2^{-\Delta\Delta C}{}_T$ method.

Tsacc full-length and novel proteins display distinct localization patterns in muscle cells.

To elucidate the sub-cellular location of Tsacc in muscle cells, pEGFP-Tsacc-FL and pEGFP-Tsacc-novel expression plasmids were created and transfected into C_2C_{12} cells. Tsacc-FL displayed localization that was specific to the cytoplasm and was nuclear excluded (Fig. 11), while the Tsacc-novel displayed a diffuse pattern, localizing in both the cytoplasm and the nucleus (Fig. 12). These distinct localization patterns are likely due to the 49 amino acid region that is missing in the Tsacc-novel isoform.

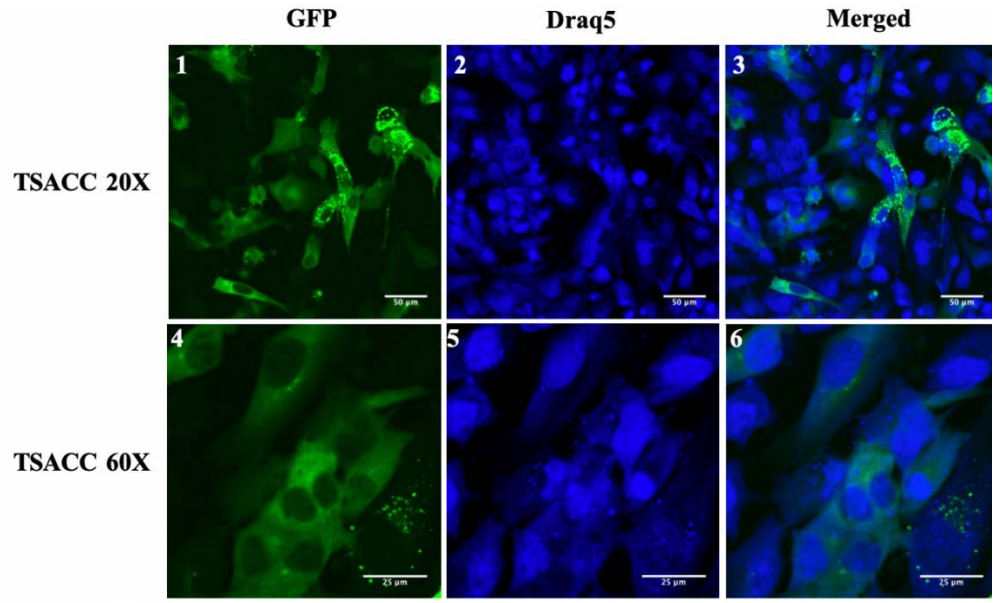

Figure 11. **Tsacc-FL localizes to the cytoplasm of muscle cells**. C_2C_{12} cells transfected with full length Tsacc-GFP displayed cytoplasmic localization (Panels 1 and 4). Cells transfected with full-length Tsacc-GFP were stained with Draq5 nuclear stain, visualizing the nuclei of proliferating myoblasts (Panels 2 and 5). Overlay of Draq5 stained and full-length Tsacc-GFP expressing cells displayed nuclear exclusion of Tsacc in muscle cells (Panels 3 and 6).

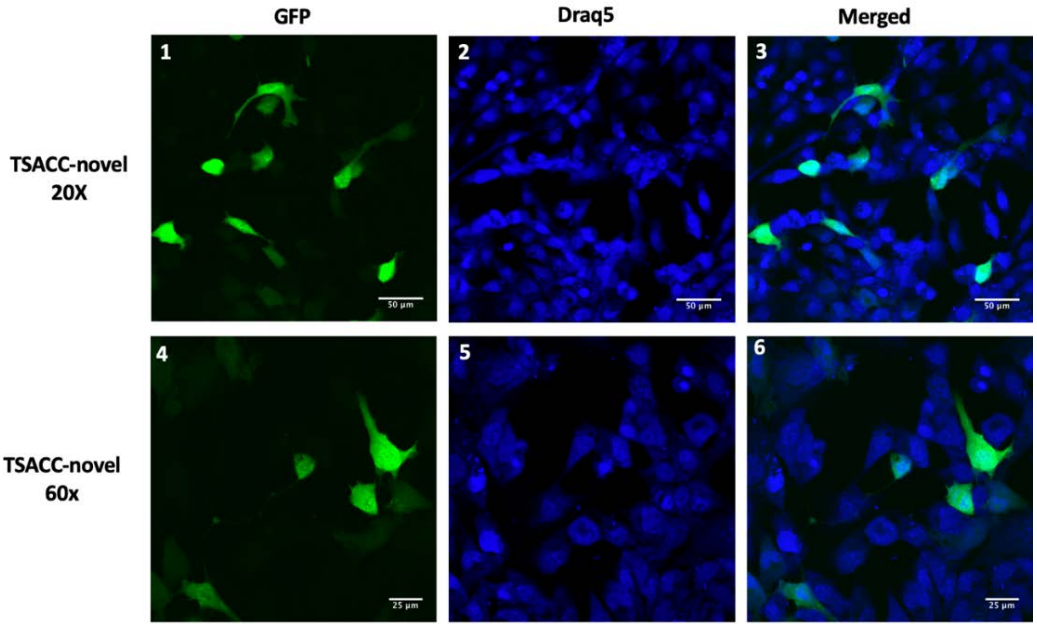

Figure 12. Tsacc-novel localizes to both the cytoplasm and nucleus of muscle cells. C_2C_{12} cells transfected with novel Tsacc-GFP displayed cytoplasmic localization (Panels 1 and 4). Cells transfected with novel Tsacc-GFP and stained with Draq5 nuclear stain, visualizing the nuclei of proliferating myoblasts (Panels 2 and 5). Overlay of Draq5 stained and novel Tsacc-GFP expressing cells displayed both cytoplasmic and nuclear localization of the novel Tsacc protein in muscle cells (Panels 3 and 6).

Ectopic expression of Tsacc-FL attenuates muscle cell differentiation while Tsacc-novel overexpression has no effect on muscle cell differentiation.

To better characterize the role of Tsacc in skeletal muscle, a myc-tagged Tsacc expression plasmid was constructed and used in all Western blot analyses due to the novelty of this gene and the unavailability of a commercial antibody. In frame fusion of the Tsacc cDNA with the myc tag was confirmed by sequencing and overexpression in C_2C_{12} cells using the myc-tagged pCS2(+)-myc-Tsacc-FL and pCS2(+)-myc-Tsacc-Novel expression plasmids. Protein was then isolated from transfected cells and Western blot analysis was performed using increasing concentrations (25µg, 50µg, and 75µg) of protein homogenates isolated from the Tsacc overexpressing cells and membranes were probed for myc-tagged Tsacc using an anti-myc antibody (Fig. 13).

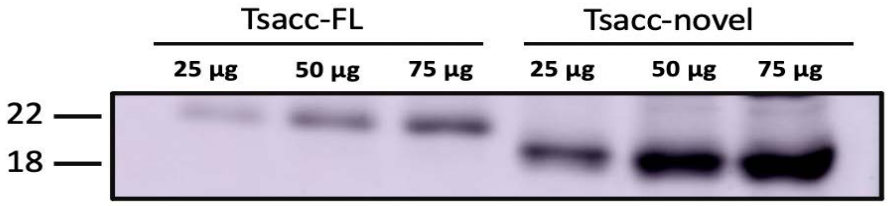

Figure 13. Validation of myc-tagged Tsacc-FL and Tsacc-novel overexpression in C2C12 cells. C_2C_{12} cells were transfected with a myc-tagged Tsacc-FL or myc-tagged Tsacc-novel expression plasmid and Tsacc overexpression was confirmed by probing with an anti-myc antibody.

To evaluate if Tsacc impacts muscle cell differentiation, C_2C_{12} cells transfected with myc-tagged Tsacc-FL or myc-tagged Tsacc-novel expression plasmids were harvested over a time course that included 2 days of proliferation (PD2) and 1, 3, and 5 days of differentiation (DD1, DD3, and DD5, respectively). Protein was isolated from cells and evaluated for the expression of known markers of muscle cell differentiation, including myosin heavy chain (MyHC) and myogenin. Western blot analysis revealed that Tsacc-FL overexpression significantly decreased

both myogenin and MyHC expression at all differentiation timepoints (Fig. 14A). To verify inhibition of muscle differentiation, Tsacc-FL was overexpressed in biological quadruplicates and harvested at 3 days post-differentiation. Lysates were evaluated by Western blot and myogenin and MyHC expression levels were found to be significantly repressed in lysates isolated from cells ectopically expressing Tsacc-FL (Fig. 14B). Interestingly, overexpression of Tsacc-Novel in muscle cells appears to have very little effect on either MyHC or myogenin levels (Fig. 15A). This observation was further examined by overexpressing Tsacc-novel in biological quadruplicates and harvesting C_2C_{12} cells at differentiation day 1. Lysates were evaluated by Western blot and myogenin expression levels were not found to be significantly repressed in lysates isolated from cells ectopically expressing Tsacc-novel (Fig. 15B) Tsacc-novel effects on MyHC were not analyzed in the quadruplicates at differentiation day 1, since MyHC expression is usually very low during early differentiation (Fig. 15B). All blots were Ponceau S stained prior to probing to confirm transfer efficiency and equal protein loading (Fig. 14 and 15). GAPDH protein levels were also analyzed to confirm that protein levels were equally loaded for all samples (Fig. 14 and 15).

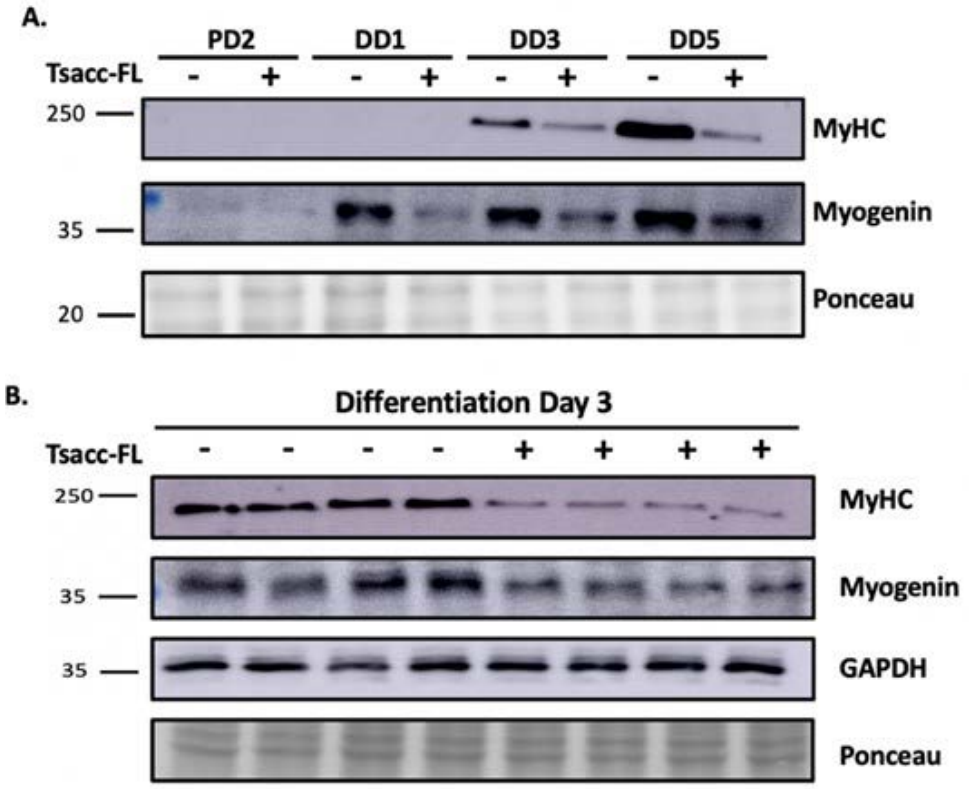

Figure 14. Ectopic expression of Tsacc-FL attenuates muscle cell differentiation. C_2C_{12} cells were transfected with the pCS2(+)-myc-Tsacc-FL expression plasmid. Cells were maintained in media supplemented with 10% serum for the proliferation timepoints and switched to DMEM supplemented with 2% serum to induce differentiation. Cells were harvested at proliferation day 2 (PD2) and differentiation days 1, 3, and 5 (DD1, DD3, DD5). (A) Western blot analysis of the differentiation markers Myosin Heavy Chain (MyHC) and myogenin showed significantly lower levels of expression at DD3 and DD5 in response to Tsacc-FL overexpression. (B) Western blot analysis of MyHC and myogenin using protein homogenates from C_2C_{12} cells differentiated for 3 days. C_2C_{12} cells were transfected with the myc-tagged Tsacc-FL expression plasmid in biological quadruplicates, maintained in proliferation media, and then switched to differentiation media (2% serum) for 3 days.

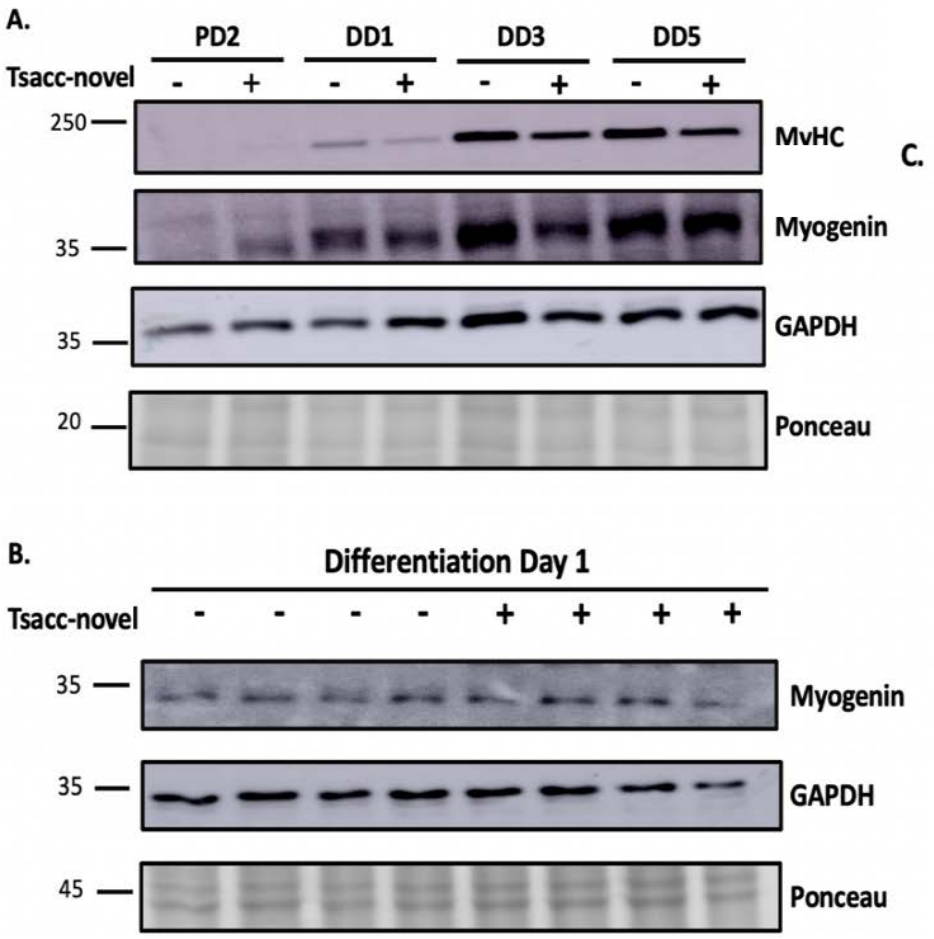

Figure 15. Ectopic expression of Tsacc-novel does not appear to affect muscle cell differentiation. C_2C_{12} cells were transfected with a pCS2(+)-myc-Tsacc-novel expression plasmid. Cells were maintained in DMEM supplemented with 10% serum for the proliferation timepoints and switched to DMEM supplemented with 2% serum to induce differentiation. Cells were harvested at proliferation day 2 (PD2) and differentiation days 1, 3, and 5 (DD1, DD3, DD5). (A) Western blot analysis revealed no significant change in Myosin Heavy Chain (MyHC) and myogenin expression in response to Tsacc-novel overexpression. (B) C_2C_{12} cells were transfected with the myc-tagged Tsacc-novel expression plasmid in biological quadruplicates, maintained in proliferation media, and then switched to differentiation media (2% serum) for 1 day. Western blot analysis of myogenin using protein homogenates from C_2C_{12} cells at differentiation day 1.

Overexpression of Tsacc may inhibit AKT activation

The effect of Tsacc overexpression on AKT signaling was evaluated by Western blot analysis over a cell differentiation time course. Cells overexpressing either myc-tagged Tsacc-FL or myc-tagged Tsacc-novel showed a reduction in p-AKT levels (Fig 16A and 16B). Whole AKT levels

were also assessed by Western blot utilizing a mouse monoclonal antibody and the results show a small decrease in whole AKT protein levels between control cells and cells overexpressing Tsacc-FL or Tsacc-novel (Fig 16A and 16B).

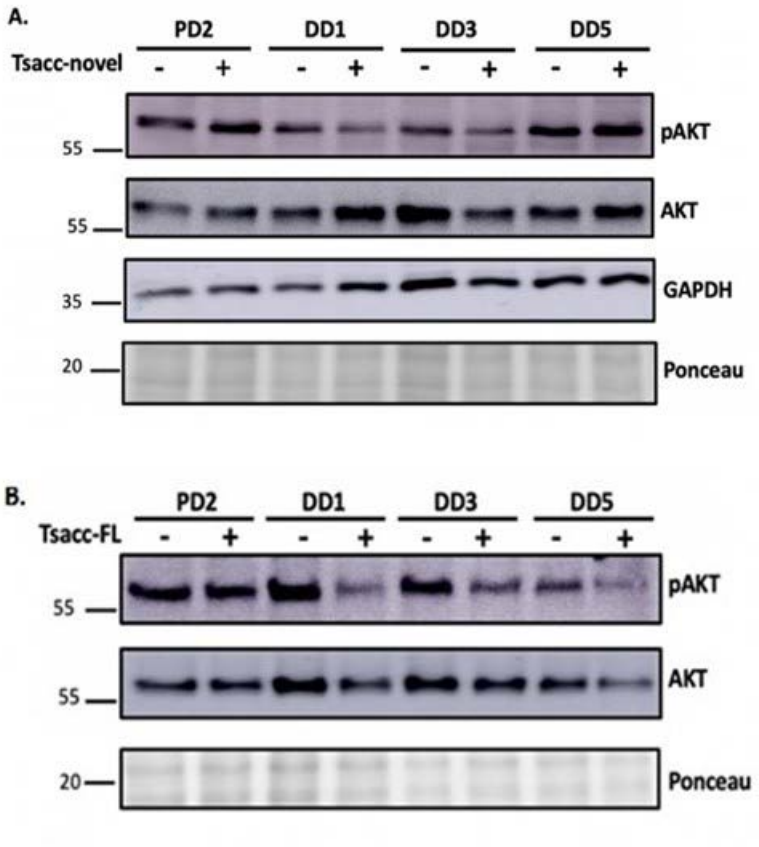

Figure 16. Ectopic expression of either Tsacc-FL or Tsacc-Novel appears to inhibit AKT activation in muscle cells. C_2C_{12} cells were transfected with either the myc-tagged Tsacc-FL or myc-tagged Tsacc-novel expression plasmids and harvested at proliferation day 2 (PD2) and differentiation days 1, 3, and 5 (DD1, DD3, DD5). (A) Western blot analysis showed a reduction in phosphorylated AKT with Tsacc-FL overexpression at all differentiation timepoints. (B) Western blot analysis showed a reduction in phosphorylated AKT with Tsacc-novel overexpression at DD1 and DD3.

Discussion

Previous studies have focused on the characterization of Tsacc in spermatids as it is believed to play a vital role in mammalian spermatogenesis. Characterization of Tsacc and its relation to skeletal muscle atrophy became of interest after the microarray data revealed differential gene expression patterns between control and denervated muscle (Furlow et al., 2013). Tsacc expression appeared to be unchanged in both wild-type and MuRF1 KO mice 3 days post-denervation but was significantly induced by 14 days post-denervation, suggesting that Tsacc is induced during "long-term" neurogenic atrophy (Fig. 7).

This investigation is the first study to characterize Tsacc in the context of skeletal muscle. While cloning the Tsacc gene from cultured muscle cells for its characterization, a novel transcript of Tsacc was identified. This transcript is 49 amino acids shorter than the full length (FL) Tsacc protein and has not been previously identified (Fig. 9). The identification of this novel transcript altered the objective of this study to not only characterize Tsacc role in skeletal muscle but to also determine whether alternative splicing altered protein function. Therefore, both full length (FL) and novel transcripts were further studied, and differences were evaluated.

Tsacc expression was evaluated through RT-qPCR analysis of C_2C_{12} myoblast. Data from these experiments showed that Tsacc mRNA expression levels increased as muscle cells underwent differentiation, with the highest expression levels occurring during late differentiation (DD7) and the lowest expression occurring during proliferation (PD2) (Fig. 10). Additionally, using a reporter gene system, Tsacc was confirmed to be transcriptionally active in skeletal muscle and was shown to be highly inducible by myogenic regulatory factors (MRFs), specifically MyoD. MRF's modulate activity of muscle-specific genes through binding of Ebox elements. Bioinformatic analysis of the Tsacc proximal regulatory region resulted in the identification of four potential

MyoD binding sites located in the proximal promoter region of Tsacc (Fig. 8). MyoD, along with myogenin, act as important biomarkers of muscle cell commitment and differentiation and are upregulated during myogenesis and neurogenic skeletal muscle atrophy (Hernandez et al., 2017, Furlow et al., 2013). This further supports our findings that Tsacc increases in expression during differentiation is likely due to regulation by MRFs, suggesting that Tsacc expression is sensitive to changes in the muscle cell environment.

The relationship between MRFs and Tsacc was further evaluated through Western blot analysis. Tsacc FL overexpression was shown to have an inhibitory effect on muscle cell differentiation, seen by a reduction in both myosin heavy chain (MyHC) and myogenin protein levels in cells overexpressing the FL transcript of Tsacc (Fig. 14). Interestingly, this inhibition of differentiation was not observed in cells that overexpressed the novel transcript of Tsacc. In cells overexpressing the novel Tsacc transcript, myogenin and MyHC protein levels appeared to be unchanged compared to control cells (Fig. 15). Although this data provides evidence that Tsacc may play a role in proper muscle cell differentiation, it also suggests a more complex interaction where alternative splicing might affect Tsacc intracellular function.

To gain better insight into Tsacc function, signal transduction pathways that are known modulators of muscle mass and size were evaluated in response to Tsacc overexpression. Since atrophying muscle tissue tend to exhibit a reduction in AKT pathway activity that is typically indicated by a reduction in phosphorylated-AKT levels, the effect of Tsacc overexpression on AKT and p-AKT levels was evaluated by Western blot analysis. The ectopic expression of Tsacc-FL or Tsacc-Novel in C_2C_{12} cells appears to negatively modulate phosphorylation levels of AKT (Fig. 16). This is interesting due to the fact previous genes characterized in our lab and identified as denervation-induced genes have also been found to modulate the AKT pathway by either

directly altering p-AKT levels or by altering the activity downstream targets such as GSK-3β or mTOR (Cooper et al., 2020b, Smith et al., 2021).

Tsacc characterization was further evaluated at the subcellular level by confocal fluorescent microscopy. Confocal microscopy revealed that Tsacc-FL localization was exclusive to the cytoplasm while the Tsacc-novel protein transcript displayed a diffuse localization pattern, exhibiting localization in both the cytoplasm and nucleus of skeletal muscle cells (Fig. 11 and 12). This data further suggests that alternative splicing plays an important role in the function of Tsacc and suggesting that the role of Tsacc in skeletal muscle might be fairly complex and dependent on which transcript is predominantly expressed. Additional research is currently underway to further characterize the role of Tsacc in the MAP Kinase and AKT signaling pathways in muscle cells.

Future Directions

Characterize the role of Tsacc in the MAP kinase signaling pathway.

The mitogen-activated protein kinase (MAPK) signaling pathway is an important pathway for muscle cell growth and development and is made up of four distinct branches, which includes extracellular signal-related kinase 1/2 (ERK1/2), p38, c-Jun N-terminal kinase (JNK), and ERK5 (Cargnello and Roux, 2011). Therefore, investigating the effect of Tsacc overexpression on MAPK signaling and determining which of these branches might be regulated by Tsacc is of particular interest. Based on previous studies from our lab, we hypothesize that Tsacc may target the ERK1/2 branch in muscle cells (Haddock et all, 2019, Hayes et al., 2019, Cooper et al., 2020a, Labuzan et al., 2020). The ERK1/2 branch modulates muscle cell development and shows variation in its activity, with ERK1/2 phosphorylation being highest during proliferation and late differentiation (Bennett and Tonks, 1997). This study suggests that Tsacc regulation of the MAPK pathway is potentially complex, with preliminary data showing that the overexpression of Tsacc-novel in

C_2C_{12} cells appears to increase p-ERK1/2 levels during proliferation and early differentiation (Fig. 17). This is of significance since it implies that Tsacc may help modulate ERK1/2 activity and regulate muscle cell differentiation, and this effect may be dependent on alternative splicing. Preliminary experiments looking at ERK1/2 activity in response to Tsacc-FL overexpression are currently underway. A potential role for Tsacc in MAP kinase signaling will also be further evaluated through the overexpression of either novel Tsacc or FL Tsacc in C_2C_{12} cells and monitoring AP-1 reporter gene activity over a time course as cells differentiate from myoblasts to myotubes.

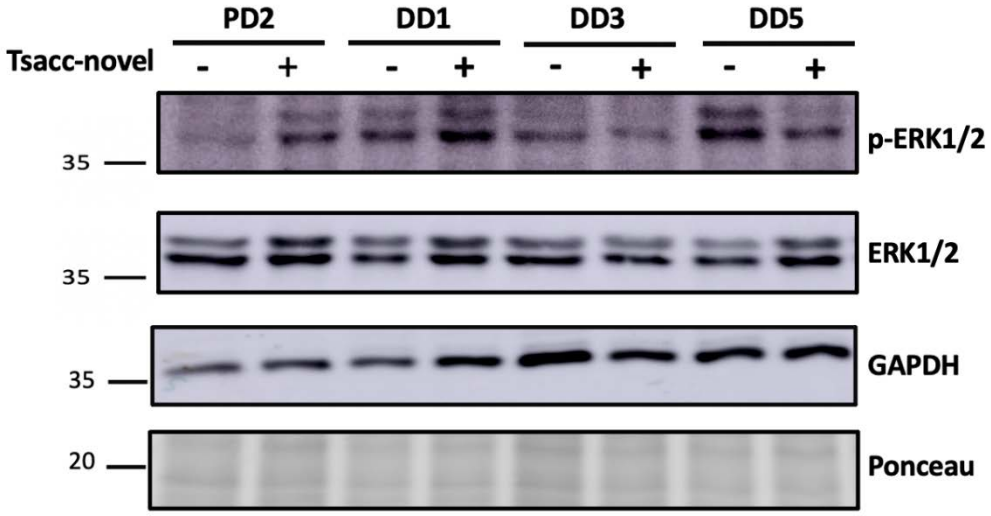

Figure 17. Ectopic expression of Tsacc-novel appears to upregulate the ERK1/2 branch of the MAPK signaling cascade. C_2C_{12} cells were transfected with the myc-tagged Tsacc-novel expression plasmid. Cells were maintained in DMEM supplemented with 10% serum for the proliferation timepoints and switched to DMEM supplemented with 2% serum to induce differentiation. Cells were harvested at proliferation day 2 (PD2) and differentiation days 1, 3, and 5 (DD1, DD3, DD5). Western blot analysis of ERK1/2 and phospho-ERK1/2 show an increase in expression at PD2 and DD1 in response to Tsacc-novel overexpression. GAPDH and Ponceau S stain were used to confirm equal protein loading across all samples.

Further analyzing the role Tsacc in MAPK signaling is of importance since it will allow for better understanding of the significance of Tsacc alternative splicing and help clarify if alternative

transcripts of Tsacc influence muscle through differential regulation of signaling pathways that are known to play an important role in muscle cell development, growth, and atrophy. To date, this study has shown that Tsacc plays a role in skeletal muscle and that its function might be more complex than originally thought due to alternative splice variants produced by this gene.

References

Aronson D, Violan MA, Dufresne SD, Zangen D, Fielding RA, Goodyear LJ. Exercise stimulates the mitogen-activated protein kinase pathway in human skeletal muscle. J Clin Invest. 1997 Mar 15;99(6):1251-7. doi: 10.1172/JCI119282. PMID: 9077533; PMCID: PMC507939.

Béchet D, Tassa A, Combaret L, Taillandier D, Attaix D. Regulation of skeletal muscle proteolysis by amino acids. J Ren Nutr. 2005 Jan;15(1):18-22. doi: 10.1053/j.jrn.2004.09.005. PMID: 15648001.

Bennett AM, Tonks NK. Regulation of distinct stages of skeletal muscle differentiation by mitogen-activated protein kinases. Science. 1997 Nov 14;278(5341):1288-91. doi: 10.1126/science.278.5341.1288. PMID: 9360925.

Bodine SC, Latres E, Baumhueter S, Lai VK, Nunez L, Clarke BA, Poueymirou WT, Panaro FJ, Na E, Dharmarajan K, Pan ZQ, Valenzuela DM, DeChiara TM, Stitt TN, Yancopoulos GD, Glass DJ. Identification of ubiquitin ligases required for skeletal muscle atrophy. Science. 2001 Nov 23;294(5547):1704-8. doi: 10.1126/science.1065874. Epub 2001 Oct 25. PMID: 11679633.

Bodine SC, Baehr LM. Skeletal muscle atrophy and the E3 ubiquitin ligases MuRF1 and MAFbx/atrogin-1. Am J Physiol Endocrinol Metab. 2014 Sep 15;307(6):E469-84. doi: 10.1152/ajpendo.00204.2014. Epub 2014 Aug 5. PMID: 25096180; PMCID: PMC4166716.

Cargnello M, Roux PP. Activation and function of the MAPKs and their substrates, the MAPK-activated protein kinases [published correction appears in Microbiol Mol Biol Rev. 2012 Jun;76(2):496]. Microbiol Mol Biol Rev. 2011;75(1):50–83. doi:10.1128/MMBR.00031-10.

Capra M, Nuciforo PG, Confalonieri S, Quarto M, Bianchi M, Nebuloni M, Boldorini R, Pallotti F, Viale G, Gishizky ML, Draetta GF, Di Fiore PP. Frequent alterations in the expression of serine/threonine kinases in human cancers. Cancer Res. 2006 Aug 15;66(16):8147-54. doi: 10.1158/0008-5472.CAN-05-3489. PMID: 16912193.

Cooper, L.M., West, R.C., Hayes, C.S., and Waddell, D.S. Dual Specificity Phosphatase 29 is Induced During Neurogenic Skeletal Muscle Atrophy and Attenuates Glucocorticoid Receptor Activity in Muscle Cell Culture. American Journal of Physiology - Cell Physiology. 2020a Aug 1; 319(2): C441-C454.

Cooper LM, Hanson A, Kavanagh JA, Waddell DS. Fam83d modulates MAP kinase and AKT signaling and is induced during neurogenic skeletal muscle atrophy. Cell Signal. 2020 Jun;70:109576. doi: 10.1016/j.cellsig.2020.109576. Epub 2020b Feb 21. PMID: 32092437.

Dave HD, Varacallo M. Anatomy, Skeletal Muscle. Statperals. 2020 Jan.

Egerman MA, Glass DJ. Signaling pathways controlling skeletal muscle mass. Crit Rev Biochem Mol Biol. 2014 Jan-Feb;49(1):59-68. doi: 10.3109/10409238.2013.857291. Epub 2013 Nov 18. PMID: 24237131; PMCID: PMC3913083.

Furlow JD, Watson ML, Waddell DS, Neff ES, Baehr LM, Ross AP, Bodine SC. Altered gene expression patterns in muscle ring finger 1 null mice during denervation- and dexamethasone-induced muscle atrophy. Physiol Genomics. 2013 Dec 1;45(23):1168-85. doi: 10.1152/physiolgenomics.00022.2013. Epub 2013 Oct 15. PMID: 24130153; PMCID: PMC3882710.

Haddock, A.N., Labuzan, S.A., Haynes, A.E., Hayes, C.S., Kakareka, K.M. and Waddell, D.S. Dual-specificity Phosphatase 4 (Dusp4) is Upregulated During Skeletal Muscle Atrophy and Modulates Extracellular Signal-Regulated Kinase (ERK) Activity. American Journal of Physiology - Cell Physiology. 2019 Apr 1; 316(4):C567-C581.

Hayes CS, Labuzan SA, Menke JA, Haddock AN, Waddell DS. Ttc39c is upregulated during skeletal muscle atrophy and modulates ERK1/2 MAP kinase and hedgehog signaling. J Cell Physiol. 2019 Dec;234(12):23807-23824. doi: 10.1002/jcp.28950. Epub 2019 Jun 12. PMID: 31188487.

Hernández-Hernández JM, García-González EG, Brun CE, Rudnicki MA. The myogenic regulatory factors, determinants of muscle development, cell identity and regeneration. Semin Cell Dev Biol. 2017 Dec;72:10-18. doi: 10.1016/j.semcdb.2017.11.010. Epub 2017 Nov 15. PMID: 29127045; PMCID: PMC5723221.

Hettmer S, Wagers AJ. Muscling in: Uncovering the origins of rhabdomyosarcoma. Nat Med. 2010 Feb;16(2):171-3. doi: 10.1038/nm0210-171. PMID: 20134473.

Hindi SM, Tajrishi MM, Kumar A. Signaling mechanisms in mammalian myoblast fusion. Sci Signal. 2013 Apr 23;6(272):re2. doi: 10.1126/scisignal.2003832. PMID: 23612709; PMCID: PMC3724417.

Hindi L, McMillan JD, Afroze D, Hindi SM, Kumar A. Isolation, Culturing, and Differentiation of Primary Myoblasts from Skeletal Muscle of Adult Mice. Bio Protoc. 2017 May 5;7(9):e2248. doi: 10.21769/BioProtoc.2248. PMID: 28730161; PMCID: PMC5515488.

Jha KN, Wong L, Zerfas PM, De Silva RS, Fan YX, Spiridonov NA, Johnson GR. Identification of a novel HSP70-binding cochaperone critical to HSP90-mediated activation of small serine/threonine kinase. J Biol Chem. 2010 Nov 5;285(45):35180-7. doi: 10.1074/jbc.M110.134767. Epub 2010 Sep 9. PMID: 20829357; PMCID: PMC2966131.

Jha KN, Tripurani SK, Johnson GR. TSSK6 is required for γH2AX formation and the histone-to-protamine transition during spermiogenesis. J Cell Sci. 2017 May 15;130(10):1835-1844. doi: 10.1242/jcs.202721. Epub 2017 Apr 7. PMID: 28389581.

Ikeda, K., Inoue, S. TRIM PROTEINS AS RING FINGER E3 UBIQUITIN LIGASES. In: Madame Curie Bioscience Database [Internet]. Austin (TX): Landes Bioscience; 2000-2013.

Jin J, Li X, Gygi SP, Harper JW. Dual E1 activation systems for ubiquitin differentially regulate E2 enzyme charging. Nature. 2007 Jun 28;447(7148):1135-8. doi: 10.1038/nature05902. PMID: 17597759.

Labuzan SA, Lynch SA, Cooper LM, Waddell DS. Inhibition of protein phosphatase methylesterase 1 dysregulates MAP kinase signaling and attenuates muscle cell differentiation. Gene. 2020 May 20;739:144515. doi: 10.1016/j.gene.2020.144515. Epub 2020 Feb 26. PMID: 32112987.

Londhe P, Davie JK. Sequential association of myogenic regulatory factors and E proteins at muscle-specific genes. Skelet Muscle. 2011 Apr 4. doi:10.1186/2044-5040-1-14

Lynch, S.A., McLeod, M.A., Orsech, H.C., Cirelli, A.M., and Waddell, D.S. Zinc Finger Protein 593 is Upregulated During Skeletal Muscle Atrophy and Modulates Muscle Cell Differentiation. Experimental Cell Research. 383(2) 2019.

McKinnell IW, Rudnicki MA. Molecular mechanisms of muscle atrophy. Cell. 2004 Dec 29;119(7):907-10. doi: 10.1016/j.cell.2004.12.007. PMID: 15620349.

Schiaffino S, Mammucari C. Regulation of skeletal muscle growth by the IGF1-Akt/PKB pathway: insights from genetic models. Skelet Muscle. 2011 Jan 24;1(1):4. doi: 10.1186/2044-5040-1-4. PMID: 21798082; PMCID: PMC3143906.

Smith AL, Gjoka E, Izhar M, Novo KJ, Mason BC, De Las Casas A, Waddell DS. FGGY carbohydrate kinase domain containing is expressed and alternatively spliced in skeletal muscle and attenuates MAP kinase and Akt signaling. Gene. 2021 Oct 20;800:145836. doi: 10.1016/j.gene.2021.145836. Epub 2021 Jul 16. PMID: 34280510.

Stitt TN, Drujan D, Clarke BA, Panaro F, Timofeyva Y, Kline WO, Gonzalez M, Yancopoulos GD, Glass DJ. The IGF-1/PI3K/Akt pathway prevents expression of muscle atrophy-induced ubiquitin ligases by inhibiting FOXO transcription factors. Mol Cell. 2004 May 7;14(3):395-403. doi: 10.1016/s1097-2765(04)00211-4. PMID: 15125842.

Wang, J., and Xia, Y. (2012). Assessing developmental roles of MKK4 and MKK7 in vitro. *Communicative & integrative biology*, *5*(4), 319–324. https://doi.org/10.4161/cib.20216

Xie, S; et al. Inhibition of the JNK/MAPK signaling pathway by myogenesis-associated miRNAs is required for skeletal muscle development. *Cell Death And Differentiation*. England, Feb. 15, 2018. ISSN: 1476-5403